Chapter 5

Ruthenium- and rhenium-diimine luminescent probes for nitric oxide synthase

Acknowledgements:

Experiments involving rhenium-diimine wires were performed in collaboration with Wendy Belliston.

ABSTRACT

Ruthenium- and rhenium-diimine based luminescent probes that bind to inducible nitric oxide synthase (iNOS) are described. The ruthenium probes have the structure $[Ru(L_2)L']^{2+}$, where L' is a perfluorinated biphenyl bridge connecting 4,4'-dimethylbipyridine to an enzyme substrate (adamantane, **1**), a heme ligand (imidazole, **2**), or F (**3**). Probe **2** binds in the active site of the murine iNOS truncation mutants Δ65 and Δ114, as demonstrated by a shift in the heme Soret from 422 to 426 nm. **1** and **3** also bind Δ65 and Δ114, as evidenced by biphasic luminescence decay kinetics. However, the heme absorption spectrum is not altered in the presence of **1** or **3**, Ru-wire binding is not affected by the presence of tetrahydrobiopterin or arginine, and the Ru to heme-Fe distances calculated from Förster energy transfer (FET) rates (~19 Å) are incompatible with binding in the iNOS dimer substrate access channel. These data suggest that **1** and **3** may instead bind to the distal side of the enzyme at the hydrophobic surface patch thought to interact with the NOS reductase domain. Novel rhenium-diimine probes with the structure [Re(4,7-dimethyl phenanthroline)$(CO)_3$L]$^+$, where L = imidazole-$C_{12}F_8$-imidazole (**4**) or imidazole-$C_{12}F_9$ (**5**) are also described. Binding of **4** to Δ114 shifts the heme Soret to 426 nm, demonstrating that the terminal imidazole functionality ligates the heme iron. Steady-state luminescence measurements show that **4** binds Δ114 with a

dissociation constant of 6 nM. The Re-wire **5** binds Δ114 with a K_d of 3.4 μM, and causes a partial displacement of water from the heme iron. Compounds with properties similar to the Ru-diimine probes may provide a novel means of NOS inhibition by preventing electron transfer between the oxidase and reductase domains. The tight binding demonstrated by **4** and the surprising ability of **5** to bind in the NOS active site suggest novel designs for NOS inhibitors. Our results demonstrate the utility of time-resolved FET measurements in the characterization of small molecule-protein interactions that are otherwise difficult to observe.

INTRODUCTION

The enzyme nitric oxide synthase (NOS) is the major biological source of nitric oxide (NO), a secondary messenger acting in a myriad of circumstances that include neuronal development, regulation of blood pressure, apoptosis, neurotransmission, and immunological response.[1-7] Because of the central importance of NO, NOS has been implicated in septic shock, inflammation, a variety of neurodegenerative disorders, and heart disease.[8-10]

The NOS oxidase domain (NOSoxy) catalyzes the conversion of arginine and molecular oxygen to NO and citrulline.[11] The electrons necessary for this reaction are provided by a reductase domain, which is attached to the oxidase domain by a calmodulin-binding linker.[12,13] NOS functions as a homodimer; the reductase domain from one half of the dimer reduces the oxidase domain of the other.[14,15] Calmodulin binding is known to modulate electron transfer, and hence catalysis.[16-18] Numerous crystal structures of NOSoxy have been determined,[19-21] but the structure of the full-length enzyme remains elusive.

We have a long-standing interest in the high-valent intermediates thought to play key roles in heme-mediated oxidations.[22-24] In order to observe these intermediates, we have designed Ru-diimine photosensitizers (Ru-wires) that bind to the mechanistically related enzyme cytochrome P450, and inject an electron into the active site upon

excitation with 470-nm light.[25] Energy transfer between the excited state of the Ru-wire and the heme also serves as a sensitive structural probe.[22,26] Given the postulated mechanistic similarities between NOS and cytochrome P450, we have endeavored to develop similar probes for NOS.

MATERIALS AND METHODS

The synthesis and characterization of the Ru-wire probes is described in appendix A. Both time-resolved and steady-state spectroscopic measurements were performed as described in chapter 1. The Stuehr lab provided samples of murine inducible NOSoxy with N-terminal truncations at residues 65 (Δ65) and 114 (Δ114). As provided, the protein samples contained millimolar concentrations of dithiothreitol, (DTT) which ligates the heme. Small aliquots of the protein solutions were exchanged into phosphate buffer (50 mM potassium phosphate, 100 mM potassium chloride) using a desalting column immediately before use. The presence of the heme Soret peak at 422 nm verified successful removal of the DTT.

High-spin, dimeric Δ65 iNOS was generated by incubating Δ65 with 1 mM tetrahydrobiopterin (H_4B) and 1 mM arginine (Arg) for 2 hours at 4 °C before diluting the sample to final concentrations of 0.1 mM H_4B and 1 mM Arg. Satisfactory Arg and H_4B binding was signaled by a shift of the Soret to 396 nm. NOS extinction coefficients were determined using the hemochromogen assay: 1 mL of NOS solution was diluted

with 0.125 mL 0.5 M NaOH and 0.125 mL pyridine, then reduced with several grains of sodium dithionite. The resulting ferrohemochromogen concentration was calculated using an extinction coefficient of 31 mM^{-1} cm^{-1} at 556 nm. The assays were calibrated using cytochrome P450cam (ε_{416} = 115 mM^{-1} cm^{-1}). The NOS extinction coefficients calculated using this method are: Δ65 ε_{422} = 75 M^{-1} cm^{-1} (substrate free and bound); substrate-free Δ114 ε_{422} = 85 M^{-1} cm^{-1}.

RESULTS

Ru-wires. In the initial stages of our investigation we tested previously developed Ru-wires (Figure 5.1) to see if any bound NOSoxy. The two murine inducible NOSoxy truncation mutants Δ114 and Δ65 were investigated in order to probe the effect of the monomer-dimer NOSoxy equilibrium. Δ114 is solely monomeric, while Δ65 exists in a monomer-dimer equilibrium, and forms a strong dimer in the presence of tetrahydrobiopterin (H_4B).[27]

No change in the NOSoxy heme absorption spectrum was observed upon the stoichiometic addition of **1** or **3** to either Δ114 or Δ65. In contrast, the addition of excess **2** to Δ65 and Δ114 resulted in a heme Soret shift from 420 and 422 to 426 nm, consist with imidazole ligation of the heme (Figures 5.2 and 5.3). The absorption spectrum of Arg- and H_4B-bound Δ65 is not altered in the presence of **1**-**3**, indicating that none of the Ru-wires displace Arg from the NOS active site.

Figure 5.1. Ru-wires. The interaction of these compounds with cytochrome P450cam is described in Chapter 2.

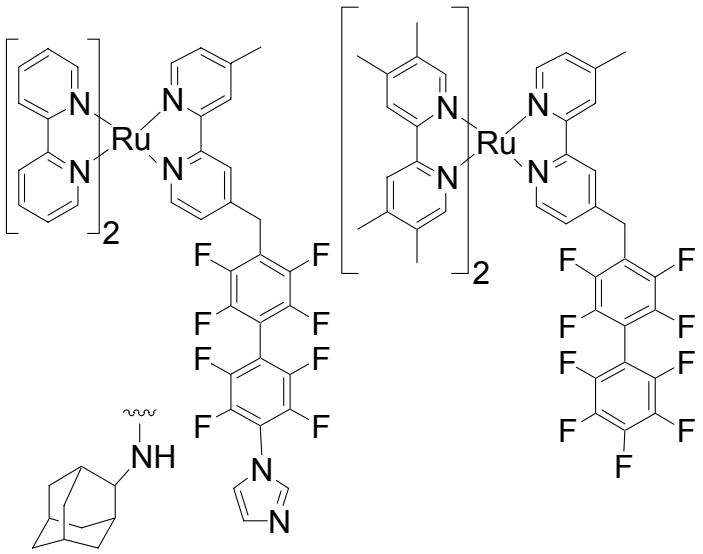

1 **2** **3**

Figure 5.2. UV-visible absorption spectrum of Δ114 alone (5.7 μM; green) and bound to **2**, corrected for the absorption due to the Ru-wire (+ 20.5 μM **2**; blue). The heme Soret peak shifts from 422 to 426 nm in response to Ru-wire binding.

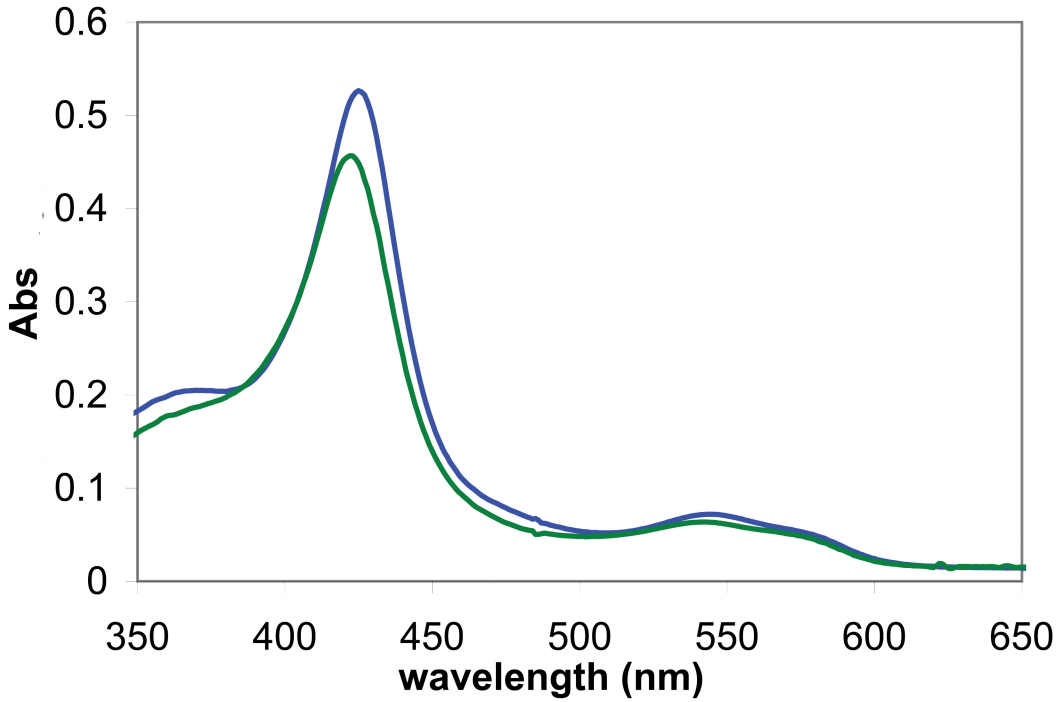
0.6
0.5
0.4
0.3
0.2
0.1
0
Abs
350
400
450
500
550
600
650
wavelength (nm)

Figure 5.3. UV-visible absorption spectrum of Δ65 alone (10 μM; green) and bound to **2** (+ 52 μM **2**; blue), corrected for absorption due to the Ru-wire. The heme Soret peak shifts from 418 to 426 nm in response to Ru-wire binding.

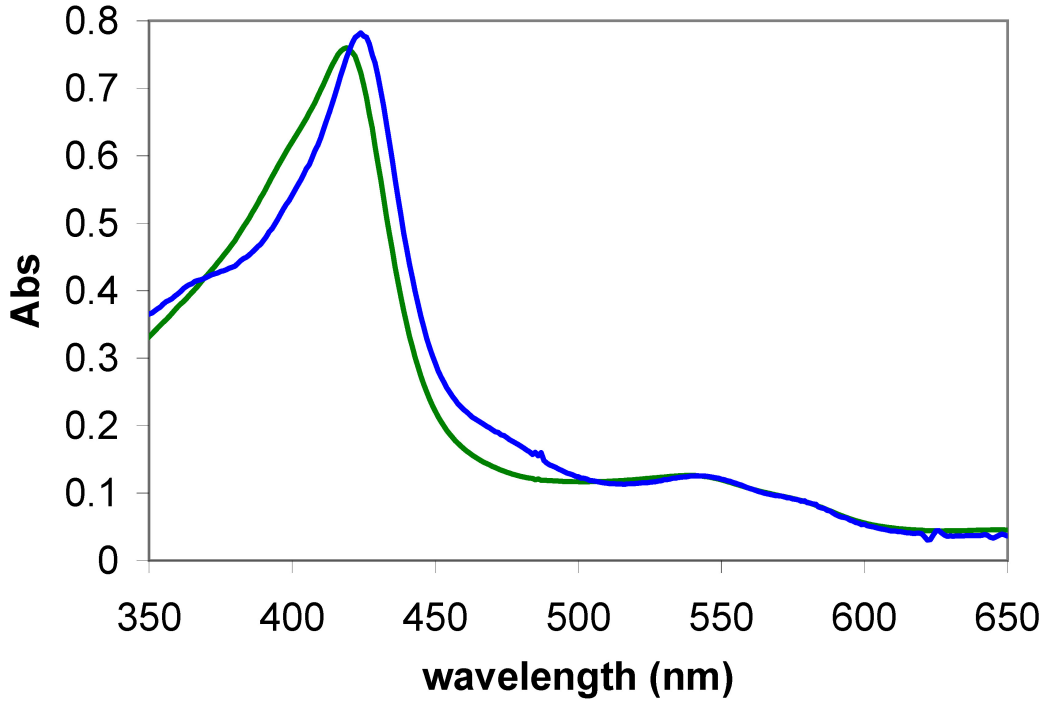
0.8
0.7
0.6
0.5
0.4
0.3
0.2
0.1
0
Abs
350
400
450
500
550
600
650
wavelength (nm)

In all cases, biexponential Ru-wire luminescence decays are observed in the presence of quantities of stoichiometic Δ114 and Δ65, indicating that the Ru-wires bind to the enzyme (Figure 5.4). As described in Chapter 2, the weightings of the fast and slow phases were used to calculate dissociation constants, while the rates of energy transfer were used to calculate Ru-heme distances. Ru-Fe distances previously calculated for Ru-wire:P450cam conjugates match those observed in the corresponding crystal structures to within 0.4 Å (Chapter 1, ref. 22).

The Ru-wires bind with micromolar dissociation constants and Ru-Fe distances of 18-21 Å (Table 1). Interestingly, the Ru-wires bind Δ114, Δ65, and H_4B- and Arg-bound Δ65 with dissociation constants that are essentially identical. The Ru-Fe distances calculated for **1** and **3** are similar for Δ114 and Δ65, and are unaffected by the presence of H_4B and Arg (Table 1). In contrast, the Ru-Fe distance calculated for the **2**:Δ144 conjugate is 17.8 Å, and increases from 19.3 to 20.9 Å upon addition of H_4B and Arg to the **2**:Δ65 conjugate, suggesting displacement from the active site.

The shifts in the absorption spectra of Δ65 and Δ114 in the presence of **2** clearly indicate that the imidazole functionality of **2** ligates the heme. In contrast, the spectroscopic evidence suggests that **1** and **3** do not bind in the active site: The heme absorption spectrum is not altered in the presence of **1** or **3**, and the K_d's and Ru-Fe distances measured with these Ru-wires are not affected by the presence of H_4B and Arg.

Figure 5.4. Sample transient luminescence data for **1** (blue) and a 1:1 mixture of **1** and Δ65 (1.8 μM; green). The fast component of the luminescence decay corresponds to **1** bound to Δ65.

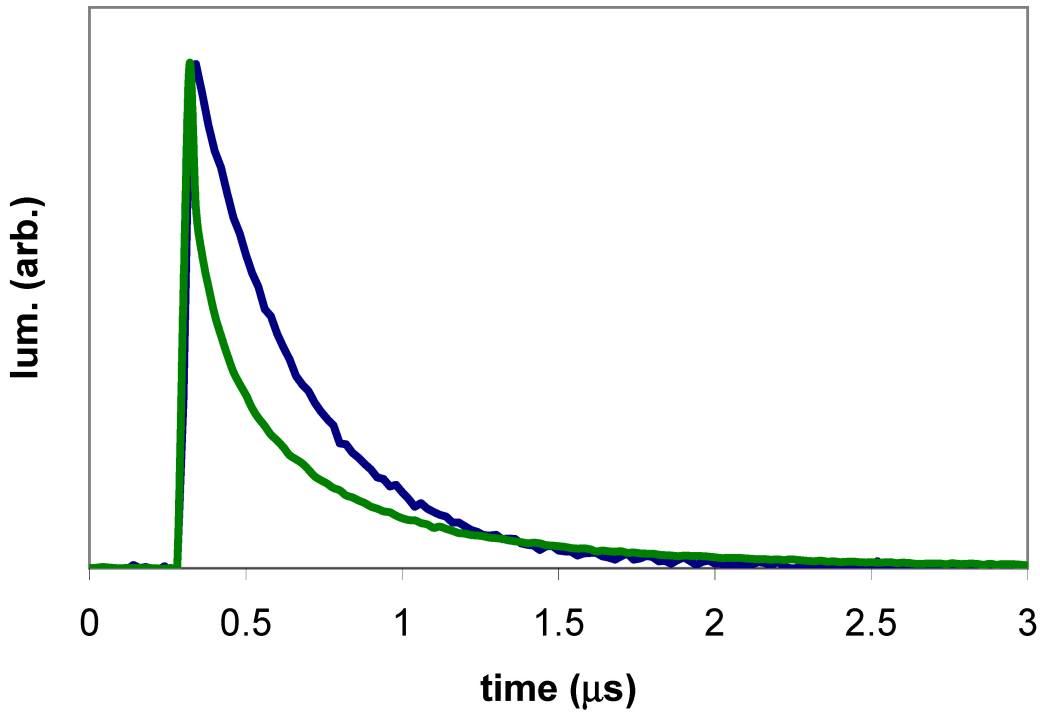
lum. (arb.)
0
0.5
1
1.5
2
2.5
3
time (μs)

Table 1. Ru-wire dissociation constants and Ru-Fe distances calculated from FET. Uncertainties are the root-mean-square deviations calculated from independent measurements (3 with Δ114, 2 with Δ65, 3 with Δ65 + Arg, + H_4B).

	Δ114		Δ65		Δ65 + Arg, +H_4B	
Compound	K_d (μM)	Ru-Fe (Å)	K_d (μM)	Ru-Fe (Å)	K_d (μM)	Ru-Fe (Å)
1	0.88 ± 0.15	18.9 ± 0.1	0.54 ± 0.04	19.6 ± 0.2	1.7 ± 0.4	19.6 ± 0.4
2	7.1 ± 0.4	17.8 ± 0.5	6.5 ± 2.4	19.3 ± 0.6	7.2 ± 3.4	20.9 ± 0.8
3	0.71 ± 0.09	20.1 ± 0.1	0.58 ± 0.16	20.2 ± 0.4	0.89 ± 0.15	21.0 ± 0.3

Structural modeling suggests that while **2** can bind to the active site of Δ114 (Figure 5.5), the Ru-wires cannot fit down the substrate access channel of dimeric NOS due to the bulk of the ruthenium *tris*-bipyridyl moiety (Figure 5.6). Instead, the Ru-Fe distances suggest that the Ru-wires may bind on the distal side of the enzyme, at the binding site of the reductase domain. This binding model is consistent with the result that the dissociation constants and Ru-heme distances of **1** and **3** are unaffected by the addition of Arg and H_4B. In addition, 1.5 equivalents of **2** bind to Δ65 when the Ru-wire is present in 6-fold excess, suggesting that **2** may bind to both the active site and another portion of the protein.

Modeling of the proposed surface binding results in Ru-heme distances consistent with those calculated from experimental data (Figure 5.6). The proposed binding site is concave and hydrophobic. The Ru-wires present few opportunities for specific interactions with the protein surface. Instead, extensive hydrophobic contacts between the Ru-wire and the protein likely provide the free energy necessary for binding. Indeed, **1** binds most tightly, while **2** is the weakest binder. This interpretation is consistent with the previously observed binding of ruthenium-diimine complexes to cytochrome *c* oxidase at the surface patch known to bind cytochrome *c*.[28,29]

Re-wires. The rhenium complexes $[Re(CO)_3(L_2)(L')]^{1+}$, where L_2 is a 2,2'-bipyridyl or

Figure 5.5. Model of **2** bound to exposed heme of Δ114. The Ru-Fe distance in this model is 16.9 Å.

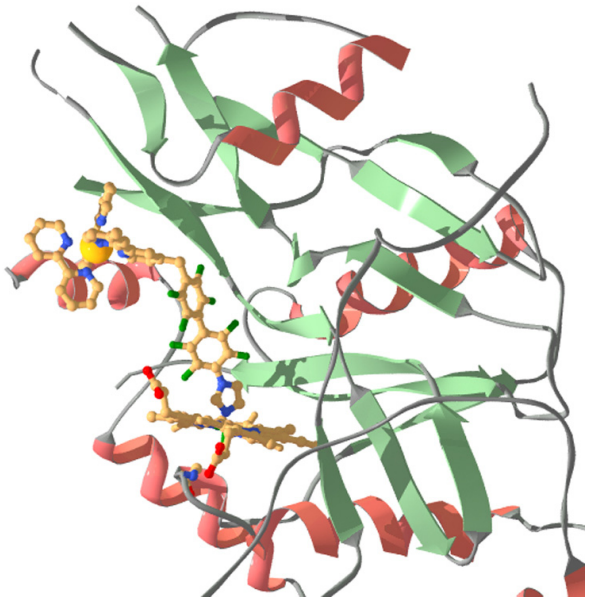

Figure 5.6. The NOS dimer, shown with $Ru(bpy)_3$ docked at the mouth of the substrate access channel (*left*), or at the proposed reductase binding site (*right*). The Ru-Fe distance is 24 Å when the Ru-diimine is bound in the substrate access channel, and ~18 Å when it is bound at the reductase domain recognition site.

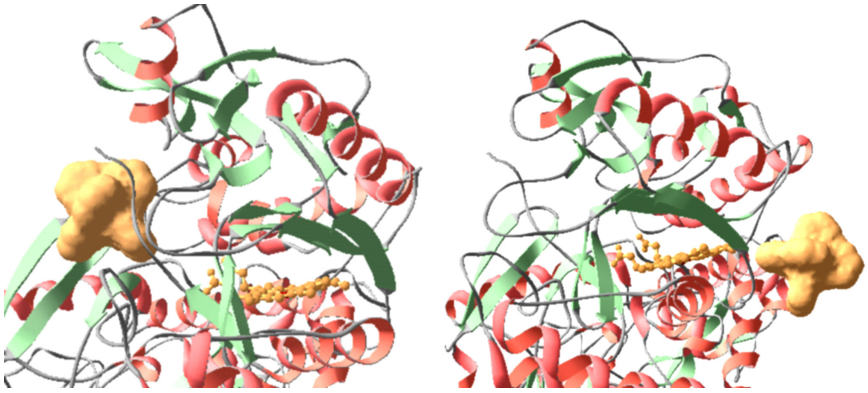

phenanthryl derivative and L' is a nitrogen donor such as imidazole or pyridine, are in general luminescent compounds with microsecond excited state lifetimes and redox properties analogous to $Ru(bpy)_3$ compounds. The excited state is both a good oxidant (1.2 V NHE) and reductant (-0.7 V NHE).[30] In addition, the photochemically generated species $[Re(CO)_3(L_2)(L')]^{2+}$ is an extremely strong oxidant (~1.8 V vs. SCE).[31]

In order to take advantage of rhenium photochemistry, compounds **4** and **5** were synthesized by Wendy Belliston (Figure 5.7). The compounds are structurally similar to **1** and **3**, but the rhenium chromophore has significantly smaller bulk. The absorption spectra of **4** and **5** are identical, and typical of Re-diimine complexes. Both are luminescent, with emission spectra centered at 560 nm and quantum yields of 0.055.

Upon addition of **4** to Δ114 murine iNOSoxy, the heme Soret absorption shifts from 422 to 426 nm, indicative of imidazole ligation to the heme iron (Figure 5.8). Time-resolved luminescence measurements indicate that **4** is almost completely bound to NOS in 1:1 micromolar solutions. A K_d could not be determined from the luminescence decay data due to the rapidity of the luminescence decay and the almost complete absence of a slow luminescence decay rate corresponding to **4** that is free in solution. Instead, a dissociation constant of 6 nM was calculated from a comparison of the steady-state luminescence spectra of **4** alone and bound to Δ114 iNOSoxy (Figure 5.9).

Figure 5.7. Re-wires. The fluorinated biphenyl bridging moieties were synthesized by reacting imidazole and perfluorobiphenyl in dimethylsulfoxide. The resulting mono- and disubstituted perfluorobiphenyl-imidazole ligands were separated by flash silica chromatography. Re(dimethylphenanthroline)$(CO)_3Cl$ was treated with silver triflate, and then reacted with either the mono- or disubstituted perfluorobiphenyl-imidazole ligand to form **4** and **5** as triflate salts.

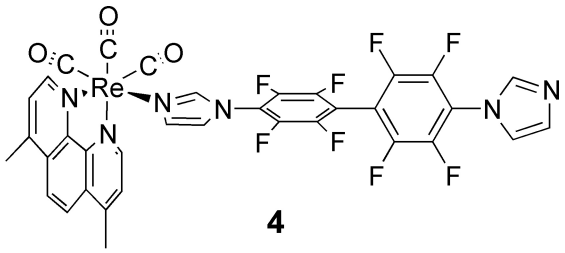

4

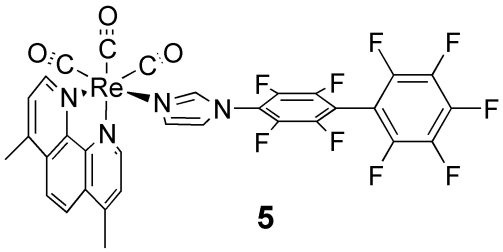

5

Figure 5.8. 10.2 μM Δ114 alone (green) and in the presence of 1 equivalent of **4**. The shift in the heme Soret is similar to that observed with **2**.

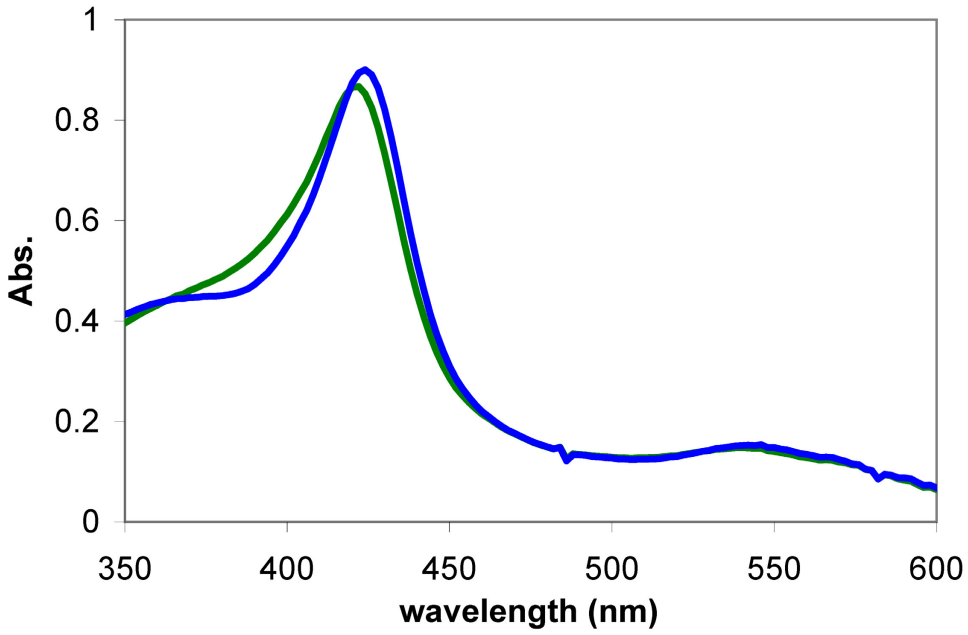
1
0.8
0.6
0.4
0.2
0
Abs.
350
400
450
500
550
600
wavelength (nm)

Figure 5.9. Steady-state luminescence spectra of 5.4 μM samples of Δ114 (black), **4** (green), and a 1:1 mixture of Δ114 and **4** (blue). The luminescence of **4** is almost completely quenched in the presence of Δ114, making it a sensitive indicator of the presence of the enzyme. Modified from a figure provided by Wendy Belliston.

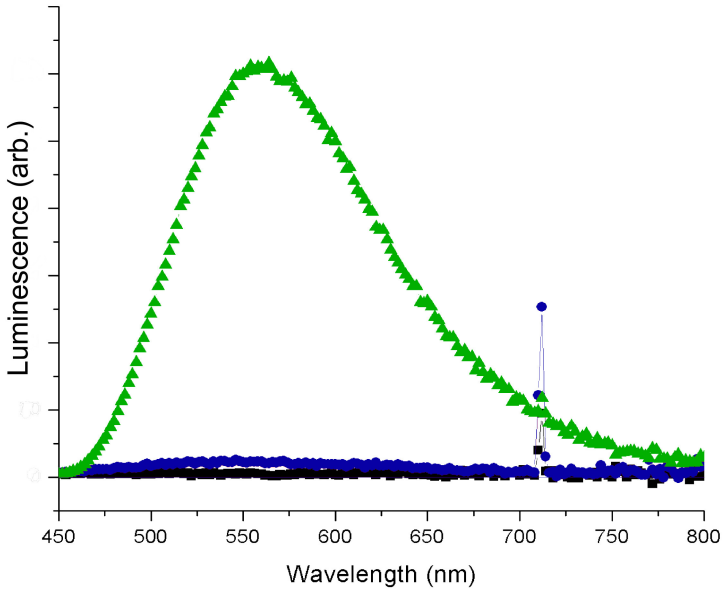
Luminescence (arb.)
450
500
550
600
650
700
750
800
Wavelength (nm)

The compound **5** causes a blue-shift in the Δ114 heme Soret, indicating a partial conversion to high-spin, 5-coordinate heme (Figure 5.10). The time-resolved luminescence decay spectra indicate that **5** binds with a dissociation constant of 3.4 μM and a Re-heme distance of ~18 Å. Both the change in the Soret absorption spectrum and the calculated Re-Fe distance are consistent with **5** binding in the active site. However, H_4B binding is also known to sometimes result in a partial low- to high-spin conversion, so binding in the pterin pocket cannot be ruled out. The structural dissimilarities of **5** and Arg make it surprising that **5** binds at all. However, the relatively exposed active site of the monomeric Δ114 iNOSoxy provides good surface complementarity with the fluorinated biphenyl moiety.

DISCUSSION

Ru-wire binding to the distal side of iNOSoxy suggests a novel method for electron injection into the active site. As with cytochrome *c* oxidase, the Ru-diimine complex likely binds to the surface of the enzyme, leaving the active site free to bind the natural substrates arginine and N-hydroxyarginine. No photoreduction was observed in the present experiments, perhaps because of the weak electronic coupling provided by the protein matrix. Future investigations employing the bimolecular photochemical generation of reduced sensitizers may circumvent this difficulty.[23]

Figure 5.10. UV-Visible absorption spectra of 6.6 μM Δ114 alone (black) and with a stoichiometric amount of **5** (red). The blue-shift in the absorption is indicative of a partial transition to high spin, five-coordinate iron.

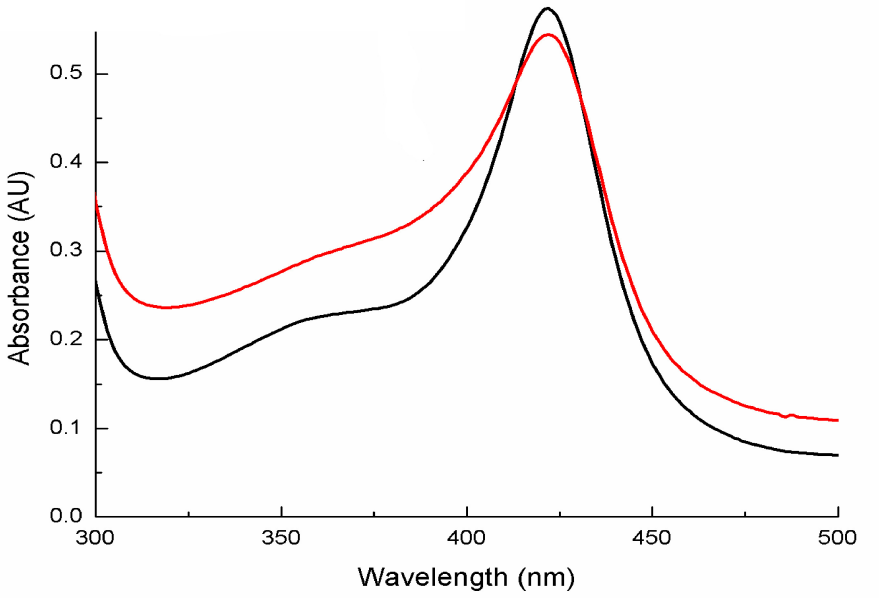
Absorbance (AU)
0.0
0.1
0.2
0.3
0.4
0.5
300
350
400
450
500
Wavelength (nm)

NOS inhibitors are being investigated as potential treatments for several diseases.[32,33] All currently known inhibitors bind in the active site of the enzyme. In contrast, Ru-wires or similar compounds may provide a novel means of NOS inhibition by preventing electron transfer (ET) between the reductase and oxidase domains. A NOS ET inhibitor would be a rare example of an inhibitor that works by preventing protein-protein interactions. Although such inhibitors are unusual, they are the subject of great interest due to the biological ubiquity and importance of transient protein complexes. These results, and other related studies (Chapter 4),[26] suggest that a conceptually simple and readily analyzed aspect of designing such inhibitors is the analysis of buried surface area in the inhibitor:protein complex.

The interactions of **2** and **4** with Δ114 are in many ways analogous to those observed with previously described inhibitors that prevent NOS holoenzyme dimerization.[34] Because only iNOS exhibits an appreciable monomer-dimer equilibrium *in vivo*, these inhibitors are highly isoform selective. The low dissociation constant of **4** makes it a useful lead compound for further iNOS inhibitor development. The three orders of magnitude difference in dissociation constants between **2** and **4** illustrates the steric influence of the $Ru(bpy)_3$ moiety.

The ability of **5** to bind in or near the NOSoxy active site is remarkable given its dissimilarity to Arg or known inhibitors. As with the Ru-wires, it seems likely that

binding is driven principally by hydrophobic interactions. Although **3** binds NOS more tightly than **5**, it does not produce a similar shift in the absorption spectrum, again demonstrating the importance of steric bulk in modulating probe-NOS interactions.

CONCLUDING REMARKS

Our results demonstrate the utility of FET measurements in characterizing small-molecule:protein interactions. Conventional UV-visible absorption measurements or competition binding assays would have overlooked the ability of **1** and **3** to bind NOSoxy. This study also shows that FET measurements can provide valuable structural information about the probe:enzyme conjugate. Similar luminescent probes may be useful in studying other heme enzymes, and more broadly proteins that emit or absorb light.

ACKNOWLEGEMENT

This research was funded by the Fannie and John Hertz Foundation (ARD) and the National Science Foundation.

REFERENCES

(1) Kendrick, K. M.; Guzman, R. G.; Zorrilla, J.; Hinton, M. R.; Broad, K. D.; Mimmack, M.; Okura, S. *Nature* **1997**, *388*, 670-674.

(2) Huang, P. L.; Huang, H. H.; Mashimo, H.; Bloch, K. D.; Moskowitz, M. A.; Bevan, J. A.; Fishman, M. C. *Nature* **1995**, *377*, 239-242.

(3) Ko, G. Y.; Kelly, P. T. *J. Neurosci.* **1999**, *19*, 6784-6794.

(4) Luth, H. J.; Holzer, M.; Gertz, H. J.; Arendt, T. *Brain Research* **2000**, *852*, 45-55.

(5) Mize, R. R.; Dawson, T. M.; Dawson, V. L.; Friedlander, M. J. *Nitric Oxide in Brain Development, Plasticity and Disease*; Elesevier, 1998.

(6) Nathan, D. *J. Clin. Invest.* **1997**, *100*, 2417-2423.

(7) Lancaster, J. *Nitric Oxide: Principles and Actions*; Academic Press: San Diego, CA, 1996.

(8) Hobbs, A. J.; Higgs, A.; Moncada, S. *Annu. Rev. Pharmacol. Toxicol.* **1999**, *39*, 191-220.

(9) Heales, S. J. R.; Bolanos, J. P.; Stewart, V. C.; Brookes, P. S.; Land, J. M.; Clark, J. B. *Biochim. Biophys. Acta-Bioenerg.* **1999**, *1410*, 215-228.

(10) Hingorani, A. D.; Liang, C. F.; Fatibene, J.; Lyon, A.; Monteith, S.; Parsons, A.; Haydock, S.; Hopper, R. V.; Stephens, N. G.; O'Shaughnessy, K. M.; Brown, M. J. *Circulation* **1999**, *100*, 1515-1520.

(11) Stuehr, D. J. *Biochim. Biophys. Acta* **1999**, *1411*, 217-230.

(12) Cho, H. J.; Xie, Q. W.; Calaycay, J.; Mumford, R. A.; Swiderek, K. M.; Lee, T. D.; Nathan, C. *J. Exp. Med.* **1992**, *176*, 599-604.

(13) Bredt, D. S.; Hwang, P. M.; Glatt, C. E.; Lowenstein, C.; Reed, R. R.; Snyder, S. H. *Nature* **1991**, *351*, 714-718.

(14) Crane, B. R.; Rosenfeld, R. J.; Arvai, A. S.; Ghosh, D. K.; S.Ghosh; Tainer, J. A.; Stuehr, D. J.; Getzoff, E. D. *EMBO J.* **1999**, *18*, 6271-6281.

(15) Siddhanta, U.; Wu, C. Q.; Abu-Soud, H. M.; Zhang, J. L.; Ghosh, D. K.; Stuehr, D. J. *J. Biol. Chem.* **1996**, *271*, 7309-7312.

(16) Kobayashi, K.; Tagawa, S.; Daff, S.; Sagami, I.; Shimizu, T. *J. Biol. Chem.* **2001**, *276*, 39864-39871.

(17) Panda, K.; Ghosh, S.; Stuehr, D. J. *J. Biol. Chem.* **2001**, *276*, 23349-23356.

(18) Abu-Soud, H. M.; Yoho, L. L.; Stuehr, D. J. *J. Biol. Chem.* **1994**, *269*, 32047-32050.

(19) Crane, B. R.; Arvai, A. S.; Gachhui, R.; Wu, C.; Ghosh, D. K.; Getzoff, E. D.; Stuehr, D. J.; Tainer, J. A. *Science* **1997**, *278*, 425-431.

(20) Raman, C. S.; Li, H. Y.; Martasek, P.; Kral, V.; Masters, B. S. S.; Poulos, T. L. *Cell* **1998**, *95*, 939-950.

(21) Poulos, T. L.; Li, H. Y.; Raman, C. S.; Schuller, D. J. In *Advances in Inorganic Chemistry, Vol 51*, 2001; Vol. 51, pp 243-293.

(22) Dmochowski, I. J.; Crane, B. R.; Wilker, J. J.; Winkler, J. R.; Gray, H. B. *Proc. Natl. Acad. Sci. USA* **1999**, *96*, 12987-12990.

(23) Wilker, J. J.; Dmochowski, I. J.; Dawson, J. H.; Winkler, J. R.; Gray, H. B. *Angew. Chem. Int. Ed. Eng.* **1999**, *38*, 90-92.

(24) Dmochowski, I. J.; Dunn, A. R.; Wilker, J. J.; Crane, B. R.; Green, M. T.; Dawson, J. H.; Sligar, S. G.; Winkler, J. R.; Gray, H. B. *Methods Enzymol.* **2002**, *357*, 120-133.

(25) Dunn, A. R.; Dmochowski, I. J.; Bilwes, A. M.; Gray, H. B.; Crane, B. R. *Proc. Natl. Acad. Sci. U. S. A.* **2001**, *98*, 12420-12425.

(26) Dunn, A. R.; Hays, A. M. A.; Goodin, D. B.; Stout, C. D.; Chiu, R.; Winkler, J. R.; Gray, H. B. *J. Am. Chem. Soc.* **2002**, *124*, 10254-10255.

(27) Ghosh, D. K.; Wu, C. Q.; Pitters, E.; Moloney, M.; Werner, E. R.; Mayer, B.; Stuehr, D. J. *Biochemistry* **1997**, *36*, 10609-10619.

(28) Zaslavsky, D.; Sadoski, R. C.; Wang, K. F.; Durham, B.; Gennis, R. B.; Millett, F. *Biochemistry* **1998**, *37*, 14910-14916.

(29) Zaslavsky, D.; Kaulen, A. D.; Smirnova, I. A.; Vygodina, T.; Konstantinov, A. A. *FEBS Lett.* **1993**, *336*, 389-393.

(30) Connick, W. B.; DiBilio, A. J.; Hill, M. G.; Winkler, J. R.; Gray, H. B. *Inorg. Chim. Acta* **1995**, *240*, 169-173.

(31) Sacksteder, L.; Zipp, A. P.; Brown, E. A.; Streich, J.; Demas, J. N.; Degraff, B. A. *Inorg. Chem.* **1990**, *29*, 4335-4340.

(32) Salerno, L.; Sorrenti, V.; Di Giacomo, C.; Romeo, G.; Siracusa, M. A. *Curr. Pharm. Design* **2002**, *8*, 177-200.

(33) Vallance, P.; Leiper, J. *Nat. Rev. Drug Discov.* **2002**, *1*, 939-950.

(34) McMillan, K.; Adler, M.; Auld, D. S.; Baldwin, J. J.; Blasko, E.; Browne, L. J.; Chelsky, D.; Davey, D.; Dolle, R. E.; Eagen, K. A.; Erickson, S.; Feldman, R. I.; Glaser, C. B.; Mallari, C.; Morrissey, M. M.; Ohlmeyer, M. H. J.; Pan, C. H.; Parkinson, J. F.; Phillips, G. B.; Polokoff, M. A.; Sigal, N. H.; Vergona, R.; Whitlow, M.; Young, T. A.; Devlin, J. J. *Proc. Natl. Acad. Sci. U. S. A.* **2000**, *97*, 1506-1511.